

This is the author's version of the work. It is posted here by permission of the AAAS for personal use, not for redistribution. The definitive version was published in Science Journal Title {VOL#366, (Oct 4)}, doi: 10.1126/science.aay1436".

A bacterial light response reveals an orphan desaturase for human plasmalogen synthesis

Authors:

**Aránzazu Gallego-García^{1*}, Antonio J. Monera-Girona^{1*}, Elena Pajares-Martínez^{1*}, Eva Bastida-Martínez¹, Ricardo Pérez-Castaño¹, Antonio A. Iniesta¹,
Marta Fontes¹, S. Padmanabhan^{2†}, Montserrat Elías-Arnanz^{1†}**

Affiliations:

¹ Departamento de Genética y Microbiología, Área de Genética (Unidad Asociada al Instituto de Química Física “Rocasolano”, Consejo Superior de Investigaciones Científicas), Facultad de Biología, Universidad de Murcia, Murcia 30100, Spain.

²Instituto de Química Física “Rocasolano”, Consejo Superior de Investigaciones Científicas, 28006 Madrid, Spain.

*These authors contributed equally to this work.

†Corresponding author. Email: melias@um.es (M.E.-A.); padhu@iqfr.csic (S.P.)

Short title:

TMEM189 is plasmanyethanolamine desaturase

Abstract:

Plasmalogens are glycerophospholipids with a hallmark *sn*-1 vinyl ether bond. These lipids are found in animals and some bacteria and have proposed membrane organization, signaling, and antioxidant roles. We discovered the plasmanylethanolamine desaturase activity essential for vinyl ether bond formation in a bacterial enzyme, CarF, which is a homolog of the human enzyme TMEM189. CarF mediates light-induced carotenogenesis in *Myxococcus xanthus*, and we found that plasmalogens participate in sensing photooxidative stress through singlet oxygen. TMEM189 and other animal homologs could functionally replace CarF in *M. xanthus*, and knocking out of TMEM189 in a human cell line eliminated plasmalogens. Discovery of the human plasmanylethanolamine desaturase will spur further study of plasmalogen biogenesis, functions, and roles in disease.

One Sentence Summary:

A long-sought enzyme essential in human plasmalogen biosynthesis is identified by studying a bacterial light response.

Main Text:

Plasmalogens are glycerophospholipids with a hydrocarbon chain linked by a vinyl ether bond at the glycerol *sn*-1 position (fig. S1, A and B) found in animals and some anaerobic bacteria, but not in plants, fungi and most aerobic bacteria, except myxobacteria (1-3). In mammals, plasmalogens are most abundant in the brain, heart and leukocytes and occur in nearly all subcellular membranes (1-3). Lipid rafts, membrane microdomain platforms proposed to recruit and activate signaling proteins (4), are enriched in plasmalogens (5, 6). The plasmalogen vinyl ether bond confers physical-chemical attributes that affect

membrane fluidity, signaling and function (1, 2) and is susceptible to cleavage by reactive oxygen species (ROS) like singlet oxygen ($^1\text{O}_2$) yielding products that may act as second messengers (7-10). Antioxidative and signaling mechanisms have thus been linked to plasmalogens, whose deficiency correlates with various human disorders including cancer and Alzheimer's disease (1, 2, 11). Mammalian plasmalogen biosynthesis involves several steps (fig. S2A) (12). A key late step in the endoplasmic reticulum (ER) converts an alkyl ether phosphatidylethanolamine (AEPE) or plasmanyethanolamine to the vinyl ether (alkenyl) phosphatidylethanolamine (VEPE) or plasmenylethanolamine (fig. S2A). This oxygen-dependent step was described almost fifty years ago (13), but the plasmanyethanolamine desaturase involved has remained an unidentified (orphan) enzyme (14, 15). In the obligately aerobic *M. xanthus* and related myxobacteria, ether lipid synthesis requires the multifunctional enzyme ElbD and, in an alternative minor pathway, MXAN_1676 (fig. S2B) (3, 16, 17). ElbD was speculated to also direct vinyl ether bond formation (16), but we have discovered that this desaturase activity corresponds to another protein, CarF, and that it is functionally conserved in animals including humans.

In *M. xanthus*, CarF signals the light response triggered by $^1\text{O}_2$ produced upon photoexcitation of protoporphyrin IX (PPIX) to somehow inactivate a membrane-associated anti- σ factor, CarR, and release its cognate σ factor, CarQ (18-21). This enables transcription of genes for the biosynthesis of carotenoids, which quench $^1\text{O}_2$ and other ROS, and provokes a yellow-to-red color change (the Car⁺ phenotype). In another pathway, light directly inactivates a B₁₂-based photoreceptor that represses genes for carotenogenesis in the dark (22-24). CarF sequence homologs exist in myxobacteria and few other bacteria (mostly Leptospiraceae and Alphaproteobacteria), in invertebrate and vertebrate animal species including humans, where they are denoted TMEM189 or Kua

and have unknown functions (19-21, 25), and in plants, with *Arabidopsis thaliana* having three (At1, At2 and At3) (fig. S3 and table S1). From phylogenetic analyses, myxobacterial and *Leptospira* CarF homologs appear more related to those in animals, and those from Alphaproteobacteria to ones in plants (fig. S3A). CarF has twelve histidines, all cytoplasmic based on its experimentally determined four-transmembrane helix topology (Fig. 1A), with five shown to be important for function thus far (19, 20). Animal CarF homologs conserve eleven of these histidines, plants eight, and bacteria eight or more (fig. S3 and table S1). To assess the functional importance of each His *in vivo* we conditionally expressed, using a vanillate-inducible system, single His-to-Ala N-terminal FLAG-tagged CarF variants in the Car⁻ *carF*-deleted ($\Delta carF$) *M. xanthus* strain. FLAG-tagged CarF is functional since cells expressing it were Car⁺, as were variants H183A and H190A and that mutated in the nonconserved His218, whereas the remaining nine His mutants were all Car⁻ (Fig. 1B). Nine histidines are therefore important in CarF function. All nine are conserved in CarF homologs from other myxobacteria, Leptospirales and animals; but one of these, His113, differs in plant (where it is often an Arg) and other bacterial homologs (fig. S3 and table S1). The HxxxH and HxxHH pattern of the functionally crucial His164/His168 and His191/His194/His195, respectively, occurs in membrane-associated diiron fatty acid desaturases and hydroxylases of otherwise low overall sequence similarity to CarF (19-21, 25). Furthermore, At3 is a chloroplast desaturase (FAD4) that generates an unusual *trans* double bond in the *sn*-2 acyl carbon chain (fig. S1C) (26). We therefore investigated if *M. xanthus* CarF is a desaturase.

Fatty acid methyl ester (FAME) analysis revealed complete absence of a peak in the $\Delta carF$ strain (Fig. 2A) that in the wild-type *M. xanthus* corresponds to iso15:0-dimethylacetal (i15:0-DMA, indicative ion $m/z=75$) derived from its plasmalogen,

MxVEPE (fig. S4) (16, 17). This i15:0-DMA peak was restored in the $\Delta carF$ strain expressing a vanillate-inducible *carF* gene (Fig. 2A), indicating that CarF is essential for the production of MxVEPE. Whether the i15:0-DMA peak reappeared when $\Delta carF$ cell extracts were incubated with pure CarF was also examined. After verifying that CarF with a C-terminal Strep tag is functional in *M. xanthus*, we expressed it in *E. coli* and affinity-purified it from the detergent-solubilized membrane fraction (fig. S5). Purified CarF, which contained two equivalents of iron (see Supplementary Methods), tended to slowly form higher order oligomers possibly detrimental to activity (fig. S5). Consequently, the $\Delta carF$ cell extract was incubated with freshly purified CarF under aerobic conditions followed by FAME analysis. Besides molecular oxygen, the desaturase activity that generates the plasmalogen vinyl ether bond requires NADPH and an electron transport chain involving cytochrome *b₅* (27), as in aerobic fatty acid desaturation (28). Hence, we included NADPH and assumed that the extract contains the other necessary components except CarF. Under these conditions, we detected an i15:0-DMA peak, albeit small (Fig. 2A), lending further support to the inference that MxVEPE formation requires CarF.

Single gene disruptions in *M. xanthus* implicated ElbD and, to a minor level, MXAN_1676, in ether lipid biosynthesis, and ElbD in the formation of a neutral alkyl (not vinyl) ether lipid that signals fruiting body development and sporulation and is synthesized only upon starvation (16, 17). Because our data implicated CarF, crucial in the response to light, to MxVEPE synthesis we investigated how in-frame gene deletions of *elbD* ($\Delta elbD$), MXAN_1676 ($\Delta 1676$) or both affected the light response. Single $\Delta elbD$ and $\Delta 1676$ deletion mutants acquired in the light a reddish color, which appeared somewhat less intense for the $\Delta elbD$ mutant than for the $\Delta 1676$ mutant or the wild-type strain, whereas the double $\Delta elbD\Delta 1676$ mutant was Car⁻ like the $\Delta carF$ strain (Fig. 2B). Consistent with this, activity in the light of a *lacZ* gene fused to the promoter of the

carotenogenic gene cluster (*carB::lacZ* reporter) was, relative to the wild type, ~60% less for the $\Delta elbD$ mutant and ~20% less for the $\Delta I676$ mutant, but at low basal levels (no photoinduction) in the $\Delta elbD\Delta I676$ mutant as in the $\Delta carF$ strain (Fig. 2B). To correlate these data with ether lipid and MxVEPE contents, and to infer the step in plasmalogen biosynthesis where CarF acts, we performed FAME analysis of each strain. Both i15:0-DMA and iso15:0-*O*-alkylglycerol bis-trimethylsilyl ether (i15:0-OAG-bisTMS, indicative ion $m/z=205$, derived from alkyl ether lipids) (fig. S4) were absent in the $\Delta elbD\Delta I676$ strain but, consistent with previous findings using single disruption mutants (16), both species were present at low levels in the $\Delta elbD$ strain and closer to wild-type levels in the $\Delta I676$ strain (Fig. 2C and fig. S6). By contrast, i15:0-OAG, yet no i15:0-DMA, was observed in the $\Delta carF$ strain (Fig. 2C). Expressing *elbD* or *MXAN_1676* in *trans* from an inducible promoter in the *Car* $\Delta elbD\Delta I676$ strain caused reappearance of ether lipids and plasmalogens, and of reddish colony color in the light (fig. S7), ruling out polar effects from the gene deletions. Consistent with the GC-MS results, direct assessment by LC-MS/MS revealed loss of MxVEPE and MxAEPE in the $\Delta elbD\Delta I676$ strains but only of MxVEPE in the $\Delta carF$ mutant (fig. S8). Thus, while *ElbD* or *MXAN_1676* enable biosynthesis of alkyl ether lipids, their conversion to the vinyl ether form requires CarF. In other words, CarF appears to be the ether lipid desaturase in plasmalogen synthesis.

Since CarF is implicated in both *M. xanthus* light-induced carotenogenesis and plasmalogen formation, we asked if the light response depends directly on plasmalogens by supplying them exogenously to the above mutant strains. We used three commercially available plasmalogens typically found in human cells, with an 18(Plasm) chain at the *sn*-1 position and an 18:1 (HsVEPE1), a 20:4 ω -6 (HsVEPE2) or a 22:6 ω -3 (HsVEPE3) chain at the *sn*-2 ester position (Fig. 3A and fig. S9). These human plasmalogens therefore

differ from *M. xanthus* MxVEPE, which has i15 chains at both positions (fig. S1B) (16, 17). Yet, all three rescued the Car⁺ phenotype when fed to the $\Delta carF$ and $\Delta elbD\Delta I676$ strains, as well as to the triple $\Delta carF\Delta elbD\Delta I676$ mutant strain (Fig. 3B and fig. S9). When fed with HsAEPE1, which is HsVEPE1 but with an *sn*-1 alkyl instead of vinyl ether bond (Fig. 3A), the CarF-containing $\Delta elbD\Delta I676$ strain became Car⁺ whereas both $\Delta carF$ strains remained Car⁻ (Fig. 3C). Moreover, FAME analysis detected 18:0 DMA and 18:0-OAG (neither natural to *M. xanthus*) in the HsAEPE1-fed $\Delta elbD\Delta I676$ mutant, but only 18:0-OAG in the $\Delta carF\Delta elbD\Delta I676$ strain (Fig. 3D). Accordingly, LC-MS/MS detected HsAEPE1 and HsVEPE1 in the double mutant, but only HsAEPE1 in the triple mutant (fig. S10). This result confirms HsAEPE1 uptake and its conversion, only if CarF is available, to HsVEPE1. Thus, CarF can produce plasmalogen from the corresponding human alkyl ether lipid, despite the latter having *sn*-1 and *sn*-2 moieties that differ from those in the likely natural precursor in *M. xanthus* (fig. S4).

Various human plasmalogens, distinct from the endogenous one, can mediate signaling in *M. xanthus* light-induced carotenogenesis, and CarF can convert a human alkyl ether lipid to its vinyl ether form. We therefore investigated if human and other eukaryotic homologs, as well as two bacterial ones (neither from myxobacteria), can functionally replace CarF in the *M. xanthus* light response and plasmalogen biosynthesis. Plasmids for vanillate-inducible expression in *M. xanthus* of codon-optimized N-terminal FLAG-tagged homologs from human, mouse, fly, worm, zebrafish (two), *A. thaliana* (three), the animal pathogen *Leptospira interrogans* and the alphaproteobacterial plant symbiont *Bradyrhizobium diazoefficiens* were constructed and each was introduced into the $\Delta carF$ strain. Among cells transformed with the eukaryotic homologs, those expressing animal homologs (41-46% identity, 56-59% similarity to CarF) (table S1) were all Car⁺, like those expressing FLAG-tagged or untagged CarF or its version (CarF₂₄₇) lacking the C-

terminal 34-residue segment absent in many homologs (Fig. 3E and figs. S3B and S11A). Cells expressing the *A. thaliana* homologs (31-33% identity to CarF and which do not conserve the functionally crucial H113 of CarF) (fig. S3B and table S1) remained Car even though these proteins were present at levels comparable to or greater than CarF₂₄₇ or the fly homolog (Fig. 3E). Consistently, light-induced *carB::lacZ* reporter activity was greater than basal levels in $\Delta carF$ strains expressing animal, but not *A. thaliana*, homologs (Fig. 3F); and in FAME analysis, the i15:0-DMA peak reappeared only in cells expressing the animal homologs (Fig. 3G and fig. S11, B and C). Of the two bacterial homologs tested, only the one more related to animal homologs, that from *L. interrogans* (43% identity to CarF), could functionally replace CarF in *M. xanthus* (fig. S12). Thus, animal TMEM189 proteins can use the endogenous *M. xanthus* ether lipid precursor, despite it being different from their natural substrates, to generate MxVEPE.

Given the above results, we further examined human TMEM189. This protein conserves eleven of the twelve histidines in CarF (fig. S3B) and single mutations of nine of these to Ala impaired function in *M. xanthus* (Fig. 4A), just as with the equivalent mutations in CarF (Fig. 1B), thus providing further evidence that the two proteins are closely related. Hence, we tested if TMEM189 is the plasmalogen ethanolamine desaturase in human plasmalogen synthesis using cell lines. For this, we obtained a HAP1 human cell line with a CRISPR/Cas9 *TMEM189* knockout to compare its ether lipid content with that of the parental cells by FAME analysis. Plasmalogens were detected as 16:0, 18:0 and 18:1-DMA peaks in the parental cells but were absent in their *TMEM189*-KO derivative, whereas their alkyl ether lipid precursors were detected as the corresponding OAG-bisTMS derivatives in both cell lines (Fig. 4B and fig. S13). Moreover, plasmalogens reappeared in the *TMEM189*-KO cells upon transient expression of EGFP-TMEM189 (fig. S14); and this functional EGFP-fused protein localized in HeLa cells to the ER (Fig.

4C), the proposed site for vinyl ether bond generation in plasmalogen biosynthesis (fig. S2A). Altogether, these results demonstrate that TMEM189 is the desaturase for human plasmalogen biosynthesis.

The findings above indicate that the $^1\text{O}_2$ response triggered by photoexcitation of PPIX mentioned earlier (21) requires plasmalogens. $^1\text{O}_2$ is known to provoke cleavage of the plasmalogen at its vinyl ether bond, yielding as breakdown products 2-monoacylglycerophosphoethanolamine (lyso-PE) and a fatty aldehyde (fig. S15) (7-10). Plasmalogen cleavage by $^1\text{O}_2$ to lyso-PE likely perturbs local membrane structure and properties, and adduct formation with the fatty aldehyde can render membrane proteins inactive (1, 2, 7). Either or both conceivably underlie the light- $^1\text{O}_2$ -plasmalogen signaling mechanism that leads to CarR inactivation, CarQ release and induction of carotenogenesis in *M. xanthus* (fig. S16), although a less likely mechanism without plasmalogen breakage cannot be excluded.

Our study reveals TMEM189 as the long-sought desaturase for animal plasmalogen biosynthesis and that its plant homologs lack this activity. It also establishes plasmalogens as crucial in a light-sensing and response pathway to counteract photooxidative stress. Identification of the plasmanylethanolamine desaturase allows direct studies of the nexus between plasmalogens, their cellular functions and diverse pathologies, which have thus far relied on targeting genes involved earlier in the biosynthetic pathway.

References and Notes

1. N. E. Braverman, A. B. Moser, Functions of plasmalogen lipids in health and disease. *Biochim. Biophys. Acta* **1822**, 1442-1452 (2012).
2. J. M. Dean, I. J. Lodhi, Structural and functional roles of ether lipids. *Protein Cell* **9**, 196-206 (2018).
3. H. Goldfine, The anaerobic biosynthesis of plasmalogens. *FEBS Lett.* **591**, 2714-2719 (2017).
4. E. Sezgin, I. Levental, S. Mayor, C. Eggeling, The mystery of membrane organization: composition, regulation and roles of lipid rafts. *Nat. Rev. Mol. Cell Biol.* **18**, 361-374 (2017).
5. L. J. Pike, X. Han, K. N. Chung, R. W. Gross, Lipid rafts are enriched in arachidonic acid and plasmalogen phospholipids and their composition is independent of caveolin-1 expression: a quantitative electrospray ionization/mass spectrometric analysis. *Biochemistry* **41**, 2075-2088 (2002).
6. C. Rodemer *et al.*, Inactivation of ether lipid biosynthesis causes male infertility, defects in eye development and optic nerve hypoplasia in mice. *Hum. Mol. Genet.* **12**, 1881-1895 (2003).
7. C. M. Jenkins *et al.*, Cytochrome c is an oxidative stress-activated plasmalogenase that cleaves plasmalogen phospholipids at the sn-1 vinyl ether linkage. *J. Biol. Chem.* **293**, 8693-8709 (2018).
8. O. H. Morand, R. A. Zoeller, C. R. Raetz, Disappearance of plasmalogens from membranes of animal cells subjected to photosensitized oxidation. *J. Biol. Chem.* **263**, 11597-11606 (1988).

9. R. A. Zoeller, O. H. Morand, C. R. Raetz, A possible role for plasmalogens in protecting animal cells against photosensitized killing. *J. Biol. Chem.* **263**, 11590-11596 (1988).
10. S. Stadelmann-Ingrand, S. Favreliere, B. Fauconneau, G. Mauco, C. Tallineau, Plasmalogen degradation by oxidative stress: production and disappearance of specific fatty aldehydes and fatty alpha-hydroxyaldehydes. *Free Radic. Biol. Med.* **31**, 1263-1271 (2001).
11. M. C. F. Messias, G. C. Mecatti, D. G. Priolli, P. de Oliveira Carvalho, Plasmalogen lipids: functional mechanism and their involvement in gastrointestinal cancer. *Lipids Health Dis.* **17**, 41 (2018).
12. N. Nagan, R. A. Zoeller, Plasmalogens: biosynthesis and functions. *Prog. Lipid. Res.* **40**, 199-229 (2001).
13. R. L. Wykle, M. L. Blank, B. Malone, F. Snyder, Evidence for a mixed function oxidase in the biosynthesis of ethanolamine plasmalogens from 1-alkyl-2-acyl-sn-glycero-3-phosphorylethanolamine. *J. Biol. Chem.* **247**, 5442-5447 (1972).
14. T. Harayama, H. Riezman, Understanding the diversity of membrane lipid composition. *Nat. Rev. Mol. Cell Biol.* **19**, 281-296 (2018).
15. K. Watschinger, E. R. Werner, Orphan enzymes in ether lipid metabolism. *Biochimie* **95**, 59-65 (2013).
16. W. Lorenzen, T. Ahrendt, K. A. Bozhuyuk, H. B. Bode, A multifunctional enzyme is involved in bacterial ether lipid biosynthesis. *Nat. Chem. Biol.* **10**, 425-427 (2014).

17. M. W. Ring *et al.*, Novel iso-branched ether lipids as specific markers of developmental sporulation in the myxobacterium *Myxococcus xanthus*. *J. Biol. Chem.* **281**, 36691-36700 (2006).
18. M. Elías-Arnanz, S. Padmanabhan, F. J. Murillo, Light-dependent gene regulation in nonphototrophic bacteria. *Curr. Opin. Microbiol.* **14**, 128-135 (2011).
19. M. Fontes, L. Galbis-Martínez, F. J. Murillo, A novel regulatory gene for light-induced carotenoid synthesis in the bacterium *Myxococcus xanthus*. *Mol. Microbiol.* **47**, 561-571 (2003).
20. L. Galbis-Martínez, M. Galbis-Martínez, F. J. Murillo, M. Fontes, An anti-antisigma factor in the response of the bacterium *Myxococcus xanthus* to blue light. *Microbiology* **154**, 895-904 (2008).
21. M. Galbis-Martínez, S. Padmanabhan, F. J. Murillo, M. Elías-Arnanz, CarF mediates signaling by singlet oxygen, generated via photoexcited protoporphyrin IX, in *Myxococcus xanthus* light-induced carotenogenesis. *J. Bacteriol.* **194**, 1427-1436 (2012).
22. M. Jost *et al.*, Structural basis for gene regulation by a B₁₂-dependent photoreceptor. *Nature* **526**, 536-541 (2015).
23. J. M. Ortiz-Guerrero, M. C. Polanco, F. J. Murillo, S. Padmanabhan, M. Elías-Arnanz, Light-dependent gene regulation by a coenzyme B₁₂-based photoreceptor. *Proc. Natl. Acad. Sci. U.S.A.* **108**, 7565-7570 (2011).
24. S. Padmanabhan, M. Jost, C. L. Drennan, M. Elías-Arnanz, A new facet of vitamin B₁₂: gene regulation by cobalamin-based photoreceptors. *Annu. Rev. Biochem.* **86**, 485-514 (2017).

25. T. M. Thomson *et al.*, Fusion of the human gene for the polyubiquitination coeffector UEV1 with *Kua*, a newly identified gene. *Genome Res.* **10**, 1743-1756 (2000).
26. J. Gao *et al.*, FATTY ACID DESATURASE4 of *Arabidopsis* encodes a protein distinct from characterized fatty acid desaturases. *Plant J.* **60**, 832-839 (2009).
27. M. L. Blank, F. Snyder, Plasmalogen Δ^1 -desaturase. *Methods Enzymol.* **209**, 390-396 (1992).
28. H. Goldfine, The appearance, disappearance and reappearance of plasmalogens in evolution. *Prog. Lipid. Res.* **49**, 493-498 (2010).

Acknowledgments: We thank Prof. Catherine L. Drennan (MIT) for critical comments on the manuscript; Dr. Daniel González-Silvera and Prof. Pedro L. Valero for advice on lipid analysis, José Antonio Madrid and Victoria López-Egea for technical assistance, and personnel at the instrumentation, sequencing, tissue culture and confocal microscopy facilities (all at the University of Murcia); and Dr. Javier Abellón-Ruiz (Newcastle University) for the exchange on membrane protein purification. **Funding:** This work was supported by grants BFU2015-67968-C2-1P and PGC2018-094635-B-C21 (to M.E.-A.) and BFU2015-67968-C2-2P and PGC2018-094635-B-C22 (to S.P.) from the Agencia Estatal de Investigación (AEI)-Spain and the European Regional Development Fund (FEDER); and by grants 19429/PI/14 and 20992/PI/18 (to M.E.-A.) from Fundación Séneca (Murcia)-Spain; Ph.D. fellowship contracts from the Ministerio de Educación y Cultura-Spain (to E.P.-M., A.J.M.-G. and E.B.-M.) and Ministerio de Economía y Competitividad-Spain (to R.P.-C.). **Author contributions:** M.E.-A. conceived the study. M.E.-A., S.P. and A.G.-G. designed experiments with input from other authors. A.J.M.-

G., E.P.-M., A.G.-G., E.B.-M., R.P.-C, M.F. and A.A. performed the experiments. All authors contributed to data analysis. A.G.-G., M.F., S.P. and M.E.-A. supervised research. S.P. and M.E.-A. acquired funding, wrote the original draft, *reviewed and edited it with input from all authors*. **Competing interests:** Authors declare no competing interests. **Data and materials availability:** All data is available in the main text or the supplementary materials, and strains and plasmids are available on request.

Supplementary Materials:

Materials and Methods

Figs. S1 to S16

Tables S1 to S3

References (29-40)

Figures

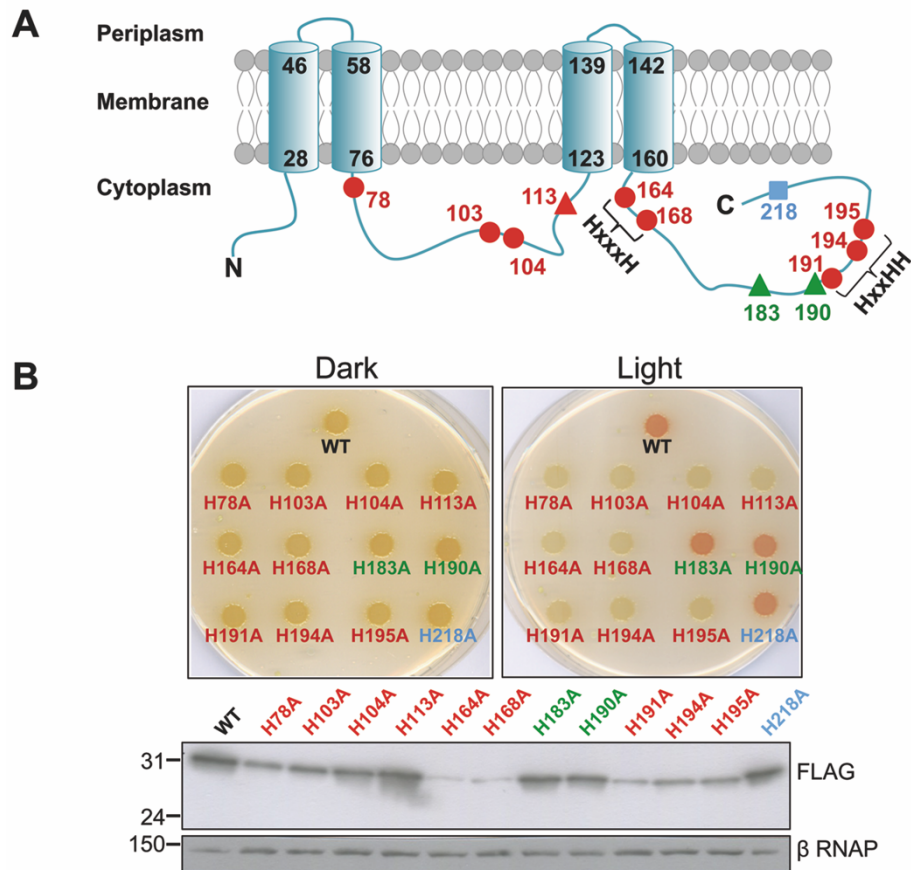


Fig. 1. *M. xanthus* CarF and histidine mutational analysis. (A) Experimentally determined membrane topology of CarF (20) and location of its twelve histidines. Numbers indicate residues in the CarF sequence. Histidines conserved in all homologs are shown as dots and those only in some homologs as triangles, and are colored according as their mutation to alanine affects (red) or not (green) CarF function. The blue square is for a nonconserved histidine. (B) Mutational analysis of histidines in CarF. Each cell spot corresponds to the *M. xanthus* $\Delta carF$ strain expressing wild-type (WT) CarF or the indicated His-to-Ala mutant version. Cells expressing a nonfunctional CarF variant

do not undergo the yellow-to-red color change when exposed to light (see Supplementary Methods). Below is a Western blot of *M. xanthus* cell extracts expressing each CarF variant probed using anti-FLAG and anti-RNAP β antibodies (as loading control).

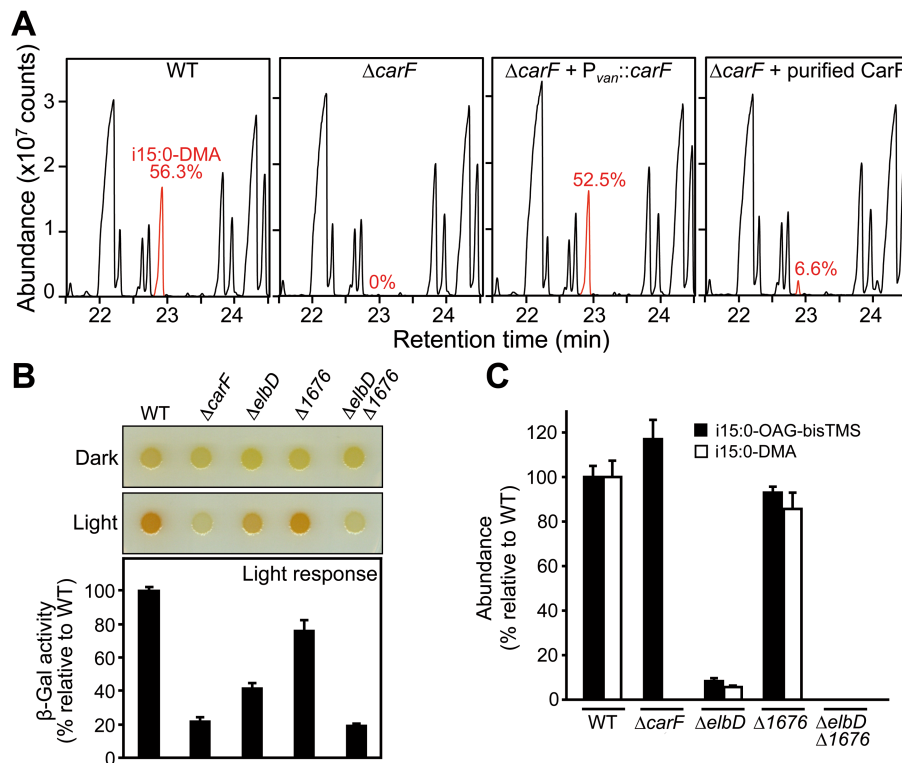


Fig. 2. CarF mediates plasmalogen synthesis in *M. xanthus*. (A) FAME GC-MS chromatogram sections of total lipid extracts from *M. xanthus* strains. i15:0-DMA peak level is shown (in %) relative to fixed amount of 17:0 internal standard. (B) Light-induced colony color assay and light-inducible *carB::lacZ* reporter probe assay (mean and standard errors, n=3; WT levels set to 100%). (C) Relative abundance of i15:0-DMA and i15:0-OAG-bisTMS (see fig. S4) for indicated *M. xanthus* strains (mean and standard errors, n=3; normalized to fixed amount of internal 17:0 standard and WT levels set to 100%).

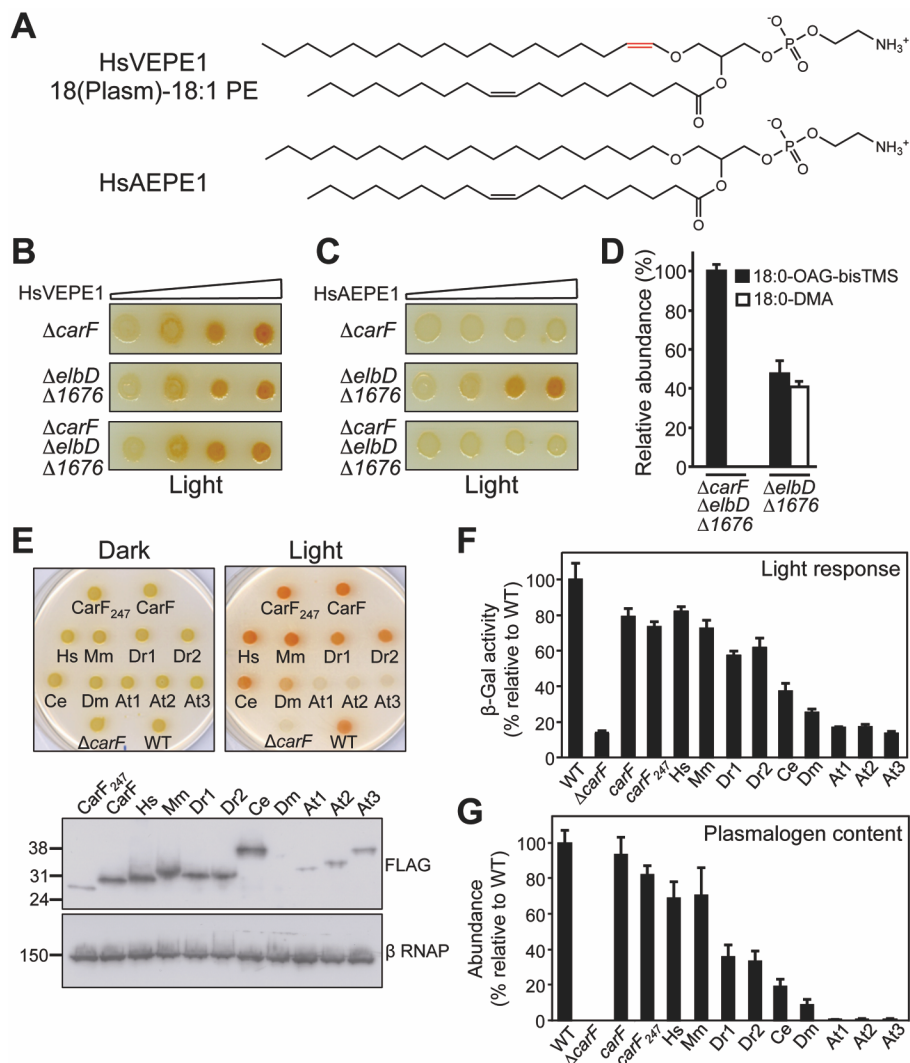


Fig. 3. Plasmalogens mediate signaling of *M. xanthus* light-induced carotenogenesis, and animal but not plant CarF homologs enable plasmalogen synthesis and light-induced carotenogenesis in *M. xanthus*. (A) HsVEPE1 and HsAEPE1 chemical structures. (B) Rescue of light-induced carotenogenesis upon feeding *M. xanthus* strains with HsVEPE1, or (C) HsAEPE1. (D) Detection of 18:0-OAG-bisTMS and 18:0-DMA in indicated *M. xanthus* strains with 17:0 as internal standard (mean and standard errors, n=3, relative to 18:0-OAG-bisTMS set to 100% in the $\Delta carF \Delta elbD \Delta 1676$ strain). (E) Light-induced colony-color assay with the $\Delta carF$ strain expressing CarF or CarF₂₄₇ (as controls) and animal (Hs, Mm, Dr1, Dr2, Ce, Dm) or plant (At1, At2, At3) CarF homologs, all N-

terminally FLAG-tagged. Western blots of the corresponding *M. xanthus* cell extracts shown below. (F) Light-inducible *carB::lacZ* reporter assay in strains used in (E). (G) Abundance of i15:0-DMA relative to internal 17:0 standard in strains used in (E). Values in (F) and (G) are mean and standard errors (n=3) relative to 100% for the WT.

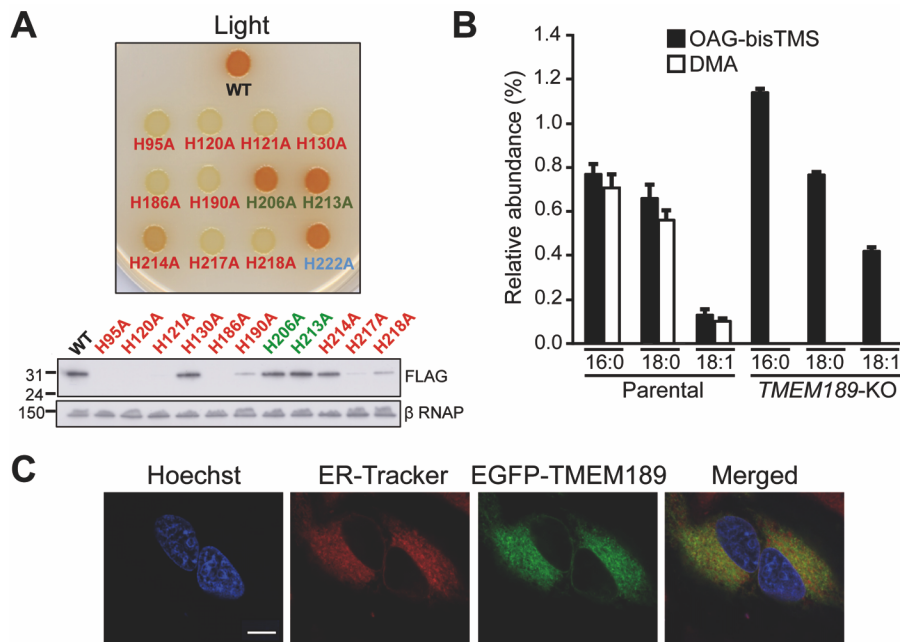


Fig. 4. Analysis of human TMEM189. (A) Mutational analysis of histidines in human TMEM189. Each spot corresponds to a $\Delta carF$ *M. xanthus* strain expressing, from a vanillate-inducible promoter, TMEM189 (WT) or the indicated His-to-Ala mutant version, all N-terminally FLAG-tagged. Mutation of the nonconserved His222 is also shown. Western blots of the corresponding *M. xanthus* cell extracts shown below. (B) Levels in the parental and *TMEM189*-KO human HAP1 cells of ether lipids and plasmalogens measured as OAG-bisTMS and DMA, respectively, by FAME GC-MS analysis (mean and standard errors relative to total, n=3). (C) Localization of human TMEM189 with an N-terminal fusion to EGFP in transfected human HeLa cells

monitored by confocal microscopy (scale bar=10 μm). ER-Tracker and Hoechst 33258 were used to image the ER and nuclear DNA, respectively.